A. Z. Hajian

R. D. Howe

Division of Engineering
and Applied Sciences,
Harvard University,
Cambridge, MA 02138

Identification of the Mechanical Impedance at the Human Finger Tip

Rapid transients were applied to the outstretched human index finger tip, which resulted in motion primarily at the metacarpophalangeal (MCP) joint in extension and in abduction. A second-order linear model was fit to approximately 20 milliseconds of the force and displacement data to determine the effective mechanical impedance at the finger tip. Ranges of mass, damping, and stiffness parameters were estimated over a range of mean finger tip force (2–20 N for extension, 2–8 N for abduction). Effective translational finger tip mass for each subject was relatively constant for force levels greater than 6 N for extension, and constant throughout the abduction trials. Stiffness increased linearly with muscle activation. The estimated damping ratio for extension trials was about 1.7 times the ratio for abduction.

I Introduction

Mechanical impedance characterizes the relationship between limb motion and externally applied task or constraint forces, and is comprised of both a static component relating forces and displacements, and a dynamic component relating forces to velocities and accelerations. Active modulation of limb impedance by the central nervous system is an essential part of effective motor control (Mussa-Ivaldi et al., 1985; Hogan, 1990). Similarly, mechanical analyses and robotic experiments have demonstrated that appropriate selection of mechanical impedance facilitates the execution of contact tasks (Whitney, 1982; Asada and Asari, 1988).

Mechanical impedance is also important in human–machine interaction, and the design of effective haptic interfaces for teleoperated systems must consider the variability of human impedance. For example, both theoretical and experimental results suggest that human operator impedance is a key factor in determining the stability and performance of haptic interfaces for teleoperated manipulation (Colgate and Brown, 1994). In the future, an understanding of human impedances and impedance-based control strategies could provide practical insight to solve problems in prosthetic limb design or in understanding neuromuscular dysfunction (Kearney and Hunter, 1982).

The primary goal of this study is to provide quantitative impedance measurements for haptic interface applications such as determining dynamic loads for mechanical design, and setting feedback gains for control system analysis. For these applications the primary interest is in the effective impedance presented by the human limb to the mechanical interface, often in a relatively unconstrained posture. This is a different emphasis from many previous studies of human limb impedance (e.g., Agarwal and Gottlieb, 1977; Crowninshield et al., 1976; Joyce et al., 1974), where the goal was to identify the impedance of a particular joint for the purpose of characterizing motor behavior.

Previous human studies of mechanical impedance include single-joint measurements of the ankle (Hunter and Kearney, 1982), elbow (Jones and Hunter, 1990a; Bennett et al., 1992), and multiarticular measurements of the arm (Hogan, 1990; Dolan et al., 1993) and leg (McMahon, 1984). Human fingers may be expected to evidence a number of important differences with these systems. First, the skeletal kinematics and musculature are more complex; most of the muscles serving the fingers are located in the lower arm and act through long tendons passing through a number of intermediate joints in the wrist and hand. In addition, the fingers must generate opposition forces against the thumb for stable grasping. These grasp forces must be controlled in concert with the net external force on the grasped object to accomplish tasks. Other complicating factors include cutaneous reflexes, particularly for grasp force control (Westling and Johansson, 1987), which are not present in other articular systems.

Because fingers have many degrees of freedom and can perform complicated and intricate tasks, and because finger impedance varies with factors such as muscle activation level, joint angle, and joint velocity, we must identify a particular task setting for any given measurement. Becker and Mote (1990) identified impedance for long time scale abduction–adduction of the index finger. Subjects maintained a near-constant contraction level based on visual feedback of surface EMG signals from the first palmar and dorsal interossei muscles, while the response to a stochastic perturbation was recorded. The authors found that a linear second-order model adequately described the system, but observed a very large day-to-day variation in fitted model parameters, perhaps due to the use of EMG signals as the basis for generating constant contraction levels. As a result of the long duration of the trials in their study, the identified impedance can include reflexes and voluntary muscular activity in response to the onset of the stimulus.

In this study we characterize and contrast the impedance at the index finger tip in extension and in abduction in a kinematic configuration used in everyday task execution. Extension is of particular interest because flexion–extension is probably the most useful degree of freedom in grasping and manipulation tasks, and because it evidences all of the complicating factors enumerated above. The records of force and acceleration in response to rapid displacements are used to fit the parameters of the linear second-order lumped element model commonly used in impedance studies. Transients with a maximum duration of 20 milliseconds were used to insure that the data were collected before the complicating contributions due to either the stretch reflex (responding to muscle length change) at approximately 30 milliseconds following the onset of a transient, or to longer latency responses such as the cutaneous slip reflex or voluntary muscle contraction. Disallowing these complicating muscular contributions permits identification of the impedance of the MCP joint independent of any sensory feedback loops. Consequently, this study of the impedance of the index finger

Contributed by the Bioengineering Division for publication in the JOURNAL OF BIOMECHANICAL ENGINEERING. Manuscript received by the Bioengineering Division March 18, 1995; revised manuscript received March 13, 1996. Associate Technical Editor: K.-N. An.

provides a baseline for future work across longer time scales, which could include the effects of reflexes and neural control activity.

II Methods

A Apparatus and Procedure. Five healthy subjects (one female, four male, ages 23–39) voluntarily participated in this study. Subjects grasped a rigid handle and rested their hand, wrist, and forearm on a rigid horizontal surface. The index finger was extended to press upon a force sensor attached to the piston of a pneumatic cylinder, which was rigidly clamped to a table (see Fig. 1). The experiment was conducted in two modes: One measured extension, and the other abduction of the index finger. The distance from the point of contact to the handle was individually set to account for finger length variations among subjects. The point of contact was the center of the finger tip pad for extension and the medial edge of the finger tip at the center of the distal phalange for abduction. Subjects were instructed to increase finger force against the apparatus gradually (mean rate 5 N/s). As the subject exceeded a variable force threshold, a solenoid valve opened, causing air to rush into the cylinder. This caused the piston to rapidly displace the tip of the fully extended index finger approximately 5 mm. Because the resulting rotational motion occurred primarily at the MCP joint, we assume that the limb mass proximal to the joint (the palm, wrist, and arm) can be considered a mechanical ground.

For extension testing, eight trials were conducted at each of six threshold levels (2–4–6–8–12–20 N) for each of the five subjects. No effects of order were observed on the identified parameters (see Results, below). For some of the subjects, 20 N approached the maximum voluntary force level in the prescribed configuration. After four of the eight trials at a given force threshold level, the threshold level was changed with the intent of minimizing anticipation as well as limiting fatigue; the order was four trials each at 4–2–12–6–8–20–8–20–6–12–2–4 N. Subjects were also permitted to pause between sets of four trials, as long as hand position was not altered until all trials were completed.

For abduction testing, eight trials were conducted at each of four threshold levels (2–4–6–8 N) for each subject. For most subjects, 8 N approached the maximum voluntary force level attainable in abduction–adduction. Tests were conducted in a similar fashion to the extension trials, with the order of force threshold levels 4–8–6–2–6–2–8–4 N.

Several additional experiments were conducted for comparative purposes, as described below. To characterize the role of finger tip pad compliance at low forces, a force threshold of 1 N was tested for each experimental mode. Similarly, to identify the effects of interphalangeal (IP) joint motion, a rigid splint was also affixed to the finger of two subjects for additional extension testing at five of the six force levels (1–2–4–8–12 N). The wooden splint was tightly bound to the index finger to compress the fingerpad and prevent motion at either IP joint.

A piezoelectric accelerometer and a force sensor (with natural frequencies of 22 kHz and 70 kHz, respectively) sensed the finger tip force and acceleration. These signals were sampled at 20 kHz with a 12-bit analog-to-digital converter. The measured acceleration was numerically integrated to generate the velocity and position data for the finger tip.

To accommodate variation in finger force threshold levels (2 N–20 N), the air pressure at the valve was varied from 240 kPa at low finger tip force levels to 340 kPa for the trials at the highest. The net time for the end plate of the piston to travel through its fixed 5 mm displacement varied between 14 and 20 milliseconds. The slight voluntary ramping of the baseline force level during the course of data acquisition was subtracted from the force record by measuring the slope of the force ramp (average rate was approximately 5 N/s) prior to the onset of piston motion.

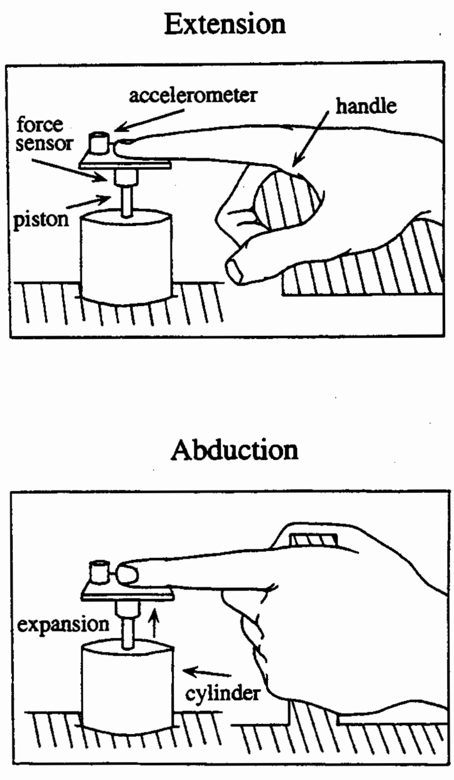

Fig. 1 Experimental apparatus

B Model and Fitting Technique. A linear second-order model

$$m\ddot{\mathbf{x}}(t) + b\dot{\mathbf{x}}(t) + k\mathbf{x}(t) = \mathbf{f}(t) \tag{1}$$

is assumed to represent the translational relationship between applied force $\mathbf{f}(t)$ and resulting displacement $\mathbf{x}(t)$, velocity $\dot{\mathbf{x}}(t)$, and acceleration $\ddot{\mathbf{x}}(t)$ of the index finger tip. The parameter m represents the effective point mass (kg), b the viscous damping (N-s/m), and k the stiffness (N/m) at the tip. Note that this lumped element translational model referred to the finger tip can be easily converted to a lumped element rotational analog about the MCP joint (Cochin and Plass, 1990) using the subjects' finger lengths (Subjects 1–5, in meters: 0.102, 0.098, 0.101, 0.090, 0.097). For the purposes of applying our findings to the design of haptic interfaces for teleoperation (e.g., Howe, 1992), we are specifically interested in the effective finger tip translational parameters.

The applied force $\mathbf{f}(t)$ and finger tip acceleration $\ddot{\mathbf{x}}(t)$ are measured with respect to an assumed zero baseline immediately prior to cylinder expansion. Only changes from this baseline affect the estimated parameters. Velocity $\dot{\mathbf{x}}(t)$ and displacement $\mathbf{x}(t)$ are similarly defined from a zero baseline. Equation (1) can be written in matrix notation as a discrete system:

$$[\mathbf{f}_i] = [\ddot{\mathbf{x}}_i\ \dot{\mathbf{x}}_i\ \mathbf{x}_i]\begin{bmatrix} m \\ b \\ k \end{bmatrix} \tag{2}$$

where $[\mathbf{f}i]$ denotes a vector of n discrete sampled values corresponding to the force transient, and $[\ddot{\mathbf{x}}_i\ \dot{\mathbf{x}}_i\ \mathbf{x}_i]$ an $(n \times 3)$ matrix of the resulting motion variables. Determination of the parameter values m, b, and k is accomplished by the division of the matrix $[\ddot{\mathbf{x}}_i\ \dot{\mathbf{x}}_i\ \mathbf{x}_i]$ by the force vector $[\mathbf{f}_i]$ to give a single least-squared error fit using the MATLAB software package. In addition, the damping ratio, defined for a second-order system as

$$\zeta = \frac{b}{2\sqrt{mk}} \tag{3}$$

is computed from the m, b, and k estimates.

To confirm the operation of the apparatus and fitting technique, the system was initially tested by expanding the cylinder with no contact while varying the mass of the endplate (5 g to 20 g), and against three different springs of known stiffness (300 N/m to 700 N/m). The measured inertial mass was always estimated to within 2.5 percent, and stiffness values were estimated to within 5.8 percent. This procedure was also used to identify both the effective moving mass of the apparatus and of the finger splint described above, each of which was subtracted from the total moving mass estimated from subjects' trials.

In preliminary experiments to confirm the invariance of the identification technique with changes in input, trials were conducted with the pneumatic pressure halved and total cylinder displacement diminished first by $\frac{1}{3}$ and then by $\frac{2}{3}$. This resulted in corresponding changes in input force levels and waveform shapes. The consequent mean identified impedance parameters at each force level were within one standard deviation of those found with the input used throughout the trials reported below, confirming the insensitivity of impedance estimates to variations in input waveform shape.

III Results

Data from a typical trial are shown in Fig. 2. Each trial begins with large peaks in both force and acceleration, indicating high inertial forces at the initial motion of the piston. The acceleration becomes negative and the velocity diminishes after approximately 10 milliseconds, due to added pneumatic resistance at the exhaust port of the cylinder because of compression of the air in the cylinder above the piston. The displacement rises steadily after the initial acceleration. The detailed shape of individual acceleration and force waveforms varied from trial to trial because of the dynamics of the pneumatic actuator. However, the preliminary experiments described above showed that even large variations in the shapes of the waveforms do not produce significant variation in impedance parameter estimates.

To illustrate the ability of the model and the fitting procedure to account for the observed behavior, a comparison of the measured and calculated forces for a typical trial is given in Fig. 3. The calculated force is computed by multiplying the kinematics matrix $[\ddot{\mathbf{x}}_i \; \dot{\mathbf{x}}_i \; \mathbf{x}_i]$ by the estimated parameter value vector $[m\; b\; k]^T$. Also shown in Fig. 3 are the inertial ($m\ddot{\mathbf{x}}_i$), damping ($b\dot{\mathbf{x}}_i$), and stiffness ($k\mathbf{x}_i$) force components that comprise the calculated force. Note that during the first few milliseconds of expansion the inertial force dominates, while in the latter part, the damping and stiffness forces become significant. The variance accounted for (VAF) by the model quantifies the quality of fit of the model (Jones and Hunter, 1990b); in this trial, the VAF is 98 percent, and the average VAF throughout the experiments is 97 percent.

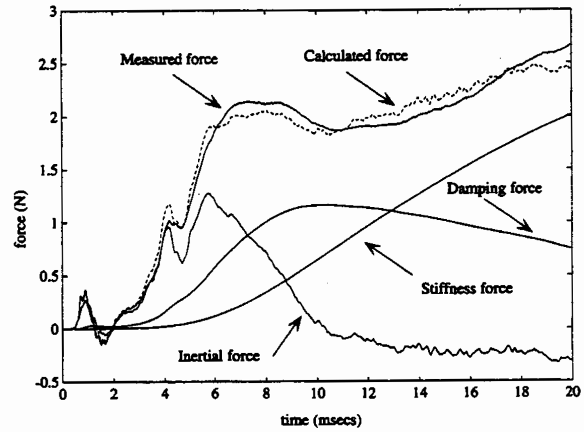

Fig. 3 Comparison of calculated and measured forces for a typical trial (6 N force, extension). In addition, the components of the calculated force are shown: the inertial force ($m\ddot{x}$), the damping force ($b\dot{x}$), and the stiffness force (kx).

The variation with force threshold of mass, damping, stiffness, and damping ratio for one subject's extension trials is shown in Fig. 4. Estimated parameter mean values and standard deviations are depicted at each force threshold level. All five subjects show similar steadily increasing damping and stiffness parameters with increasing force threshold, and a mass estimate that is relatively constant or rises to a constant plateau at force levels greater than 6 N.

Figure 5 and Table 1 show the estimated parameters for extension for all five subjects. Effective mass estimates ranged from 2.7 g to 6.7 g at 2 N, and 5.1 g to 6.7 g at 20 N. Both damping and stiffness increase nearly linearly with finger tip force, although damping has a large extrapolated zero-force value, while stiffness has a near-zero value. Damping nearly

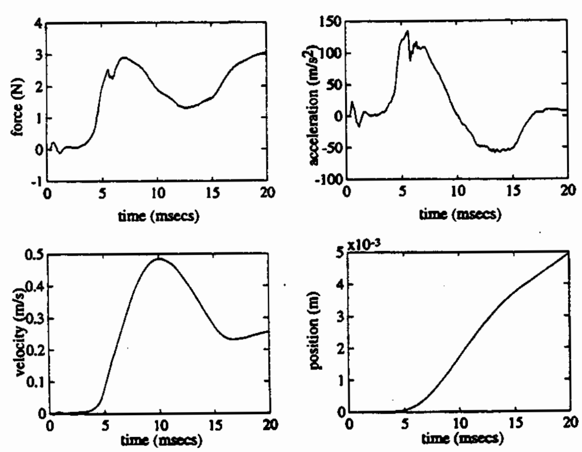

Fig. 2 Force, acceleration, velocity, and position versus time for a typical trial

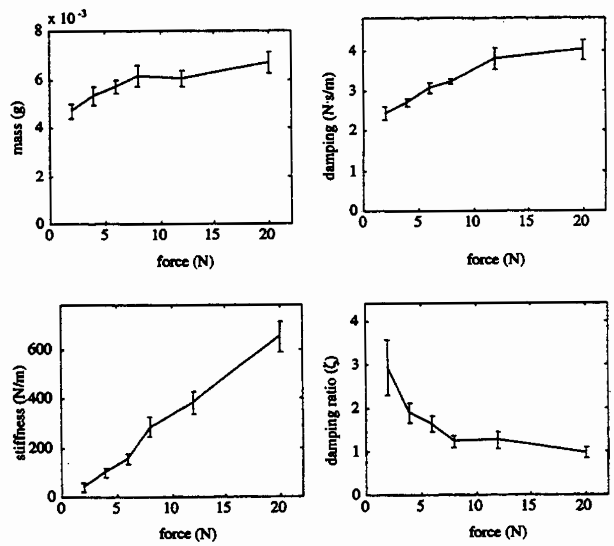

Fig. 4 Variations of the estimated mass, damping, stiffness, and damping ratio parameters in extension for one subject

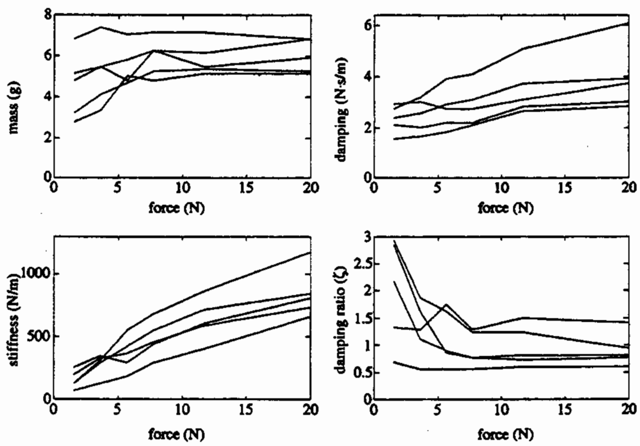

Fig. 5 Variations of the estimated mass, damping, stiffness, and damping ratio parameters in extension for all subjects

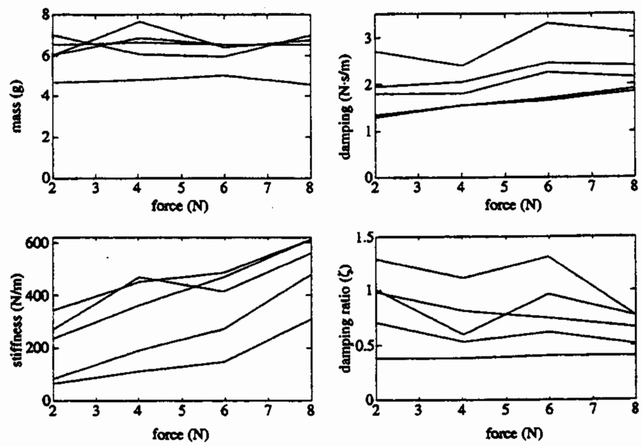

Fig. 6 Variations of the estimated mass, damping, stiffness, and damping ratio parameters in abduction for all subjects

doubled across the force range, rising from a mean of 2.2 N-s/m to a mean of 4.0 N-s/m, while stiffness rose from a mean of 200 N/m to 800 N/m across the 2 N to 20 N range. Subjects were nearly critically damped ($\zeta \approx 1$) at force levels greater than 4 N; the mean ζ at each force level ranged between 0.92 and 1.15.

Anticipation of the transient by the subjects was not a significant factor in the results. The difference in parameters estimated in the first set of four trials compared to those estimated in the second set across all force levels was not significant ($p > 0.25$). Similarly, sequences of trials for all subjects showed no training effect. There was no significant difference in parameters estimated in the first of a set of four trials as compared with parameters estimated in the other three trials ($p > 0.25$).

Figure 6 and Table 2 show parameter estimates for index finger abduction across the range of finger tip force thresholds tested (2–8 N). Mass estimates were relatively constant, ranging from 4.8 g to 7.0 g at 2 N and 8 N. Damping and stiffness estimates showed similar qualitative trends as in extension and rose with finger tip force. Damping increased from a mean of 1.84 N-s/m at 2 N to a mean of 2.27 N-s/m at 8 N, while stiffness increased from 230 N/m at 2 N to 520 N/m at 8 N.

To investigate the cause of the decreased mass estimate at low force levels in extension (Fig. 5), two subjects were fitted with splints which compressed the finger pad and prevented interphalangeal (IP) joint movement. As in the other experiments described above, eight trials were conducted at finger tip force levels of 1, 2, 4, and 12 N. Figure 7 shows the mass parameter estimate for one subject for these trials. The inertial contribution of the splint itself was measured and subtracted from the mass estimates computed in the splinted finger trials. Instead of a rising mass estimate with force level at low forces as seen in the unsplinted trials, we now see a nearly constant mass estimate at all force levels.

The damping ratio of every trial for all subjects for abduction was less than the corresponding damping ratio at the same force level for extension. Figure 8 shows the ratio of the mean ζ for all subjects ($\zeta_{extension}/\zeta_{abduction}$) at each force level from 2 to 8 N. The mean ratio is consistently greater than 1.0 across this range.

Table 1 Subjects' mean and standard deviation (std) values of the parameters m, b, k, and ζ for three of six finger tip force levels in extension

extn.	Subject	m (g)	std m	b (N-s/m)	std b	k (N/m)	std k	ζ	std ζ
	1	5.01	.653	2.86	.0855	237	25.5	1.33	.158
Force	2	6.73	.331	1.66	.140	187	40.3	.706	.143
Level	3	4.72	.308	2.45	.156	41.6	16.9	2.95	.638
2 N	4	3.20	.210	2.16	.129	108	23.3	2.20	.416
	5	2.72	.337	2.98	.154	113	43.2	2.87	.723
	1	6.09	.495	4.15	.151	422	32.7	1.30	.090
Force	2	7.00	.240	2.16	.0679	456	47.9	.573	.0297
Level	3	6.16	.439	3.23	.0711	286	40.3	1.23	.128
8 N	4	5.15	.301	2.35	.117	536	17.7	.772	.0566
	5	4.76	.292	2.80	.0922	674	32.6	.786	.0629
	1	5.85	.369	6.12	.222	614	99.4	1.41	.0948
Force	2	8.63	.337	2.91	.107	730	45.5	.617	.0397
Level	3	6.66	.433	4.02	.240	651	59.6	.970	.113
20 N	4	5.16	.266	3.11	.124	862	45.0	.804	.0602
	5	5.07	.752	3.81	.124	1189	90.3	.787	.103

IV Discussion

A Mass Estimate. Over the finger tip force range tested, the effective mass estimates for extension of each subject's finger either remained nearly constant or rose to a constant level of approximately 6 g. The diminished mass estimates seen at low finger tip force levels can be explained by a combination of two phenomena. First, at the lowest force levels, the subcutaneous finger tip pad is not yet fully compressed at the onset of piston motion (Westling and Johansson, 1987). Consequently, a millimeter or two of motion (corresponding to a significant fraction of the duration of the trial) acts to compress the finger tip pad, while the remaining motion increasingly acts to rotate the finger joints. In effect, the finger tip pad compliance approaches that of the joint being investigated, leading to a breakdown of the lumped element model, which assumes a single degree of freedom for the finger system. As a result, the overall effective mass is less than what would be estimated if the finger tip pad was compressed throughout the experiment. Data in Westling and Johansson (1987) show that this effect is most evident at the finger tip force levels below approximately 2 N (stiffness of finger tip pad ≈ 300 N/m at 0 N and greater than 3000 N/m at 2 N). At larger force levels the finger tip pad compliance diminishes to the point that we can assume finger tip pad rigidity for the purposes of the experiment.

The second factor, which results in decreased effective tip mass, is IP joint compliance. At lower force levels, the compliance at either IP joint is enough to allow some hyperextension

Table 2 Subjects' mean and standard deviation (std) values of the parameters m, b, k, and ζ for two of four finger tip force levels in abduction

abdt.	Subject	m (g)	std m	b (N-s/m)	std b	k (N/m)	std k	ζ	std ζ
	1	6.01	.214	2.68	.0546	289	32.9	1.01	.0599
Force	2	6.62	.478	1.39	.0903	364	21.6	.421	.0500
Level	3	7.03	.540	1.98	.0564	97.3	37.0	1.29	.371
2 N	4	4.78	.396	1.34	.101	117	19.0	1.00	.164
	5	6.15	.107	1.83	.0470	258	19.7	.729	.0489
	1	6.80	.464	3.07	.0674	563	27.4	.786	.0461
Force	2	6.57	.225	1.85	.105	612	38.6	.430	.0295
Level	3	7.02	.373	2.38	.109	330	49.6	.791	.0990
8 N	4	4.76	.342	1.90	.161	490	54.2	.686	.0617
	5	6.62	.338	2.17	.110	618	15.7	.538	.0385

of the joint beyond the horizontal orientation. At force levels greater than about 6 N, the finger stiffness is large enough to prevent this, and the finger behaves like a rigid body. For abduction, the estimated mass is not reduced, because the fingerpad along the medial edge of the index finger tip is not very compliant, and because the IP joints do not move in the abduction–adduction direction.

The extension trials carried out with two subjects with wooden splints verified that the low mass estimates were a result of the high finger tip pad and IP joint compliances at low force levels. The addition of the splint nullified the effects of pad and IP joint compliance, which otherwise reduce the effective mass of the finger system.

B Damping Ratio Estimate. Because the effective mass is diminished at force levels below 6 N, the identified damping ratio for the extension trials is much larger than at high force levels. In addition, the ζ from these fast transient finger extension experiments is in notable contrast to previous single joint studies, which reported a strongly underdamped response with a damping ratio in the range 0.1–0.4 (e.g., ankle flexion–extension (Hunter and Kearney, 1982), and long-term finger abduction–adduction (Becker and Mote, 1990)). A factor that may contribute to the greater damping ratio identified in this study is the preclusion of reflex responses, due to the brief duration of the trial. Although the action of these reflexes varies with task parameters, in general, they substantially increase joint stiffness, particularly the stretch reflex (e.g., Akazawa et al., 1983; Doemges and Rack, 1992). Since the damping ratio varies inversely with the square root of the stiffness, the absence of these reflexes results in a higher damping ratio. This suggests that across longer time scales, the damping ratio identified for the index finger would decrease, approaching values identified for other limbs. Further studies across larger time scales will be required to determine the magnitude of the stiffness contribution from the stretch reflex in this configuration.

Several biomechanical factors may influence the difference in the relative magnitude of the damping ratio identified for extension and for abduction as seen in Fig. 8. The unique physiology of the fingers acting in flexion–extension may increase the damping ratio of the fingers in extension. Many of the previously analyzed joints, such as the elbow, are served by muscles adjacent to the joint with relatively short tendons. Likewise, abduction–adduction of the MCP joint is actuated by the interossei muscles that are intrinsic to the hand and have correspondingly short tendons. In contrast, flexion–extension of the MCP joint is actuated principally by the flexors digitorum superficialis and profundus and the extensors digitorum and indicis, located in the forearm. The tendons through which these

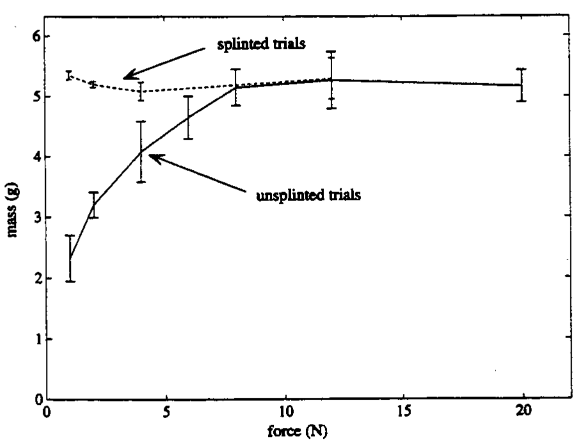

Fig. 7 Comparison of mass estimate for splinted versus unsplinted extension trials for one subject. Means and standard deviations for each set of eight trails at each force level are depicted.

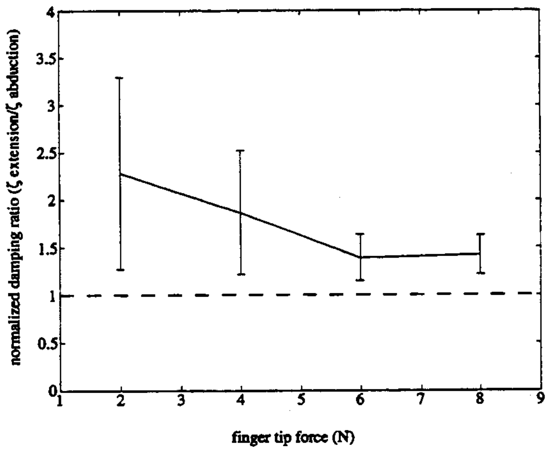

Fig. 8 Normalized damping ratio ($\zeta_{extension}/\zeta_{abduction}$) across force range shared by extension and abduction. Note that normalized ratio is always >1.

muscles act pass through the carpal tunnel and palm, which may produce additional passive damping. Another reason for the large identified damping ratio may be the compliance of the tendons themselves. At the force levels in this study, tendon stiffness may make a significant contribution to the identified finger tip stiffness (Amis, 1994). This would add another degree of freedom between the finger tip and the muscle. The finger tip pad can also be expected to provide additional damping at the contact of the apparatus, although this effect should be small above about 2 N. A more elaborate model would be required to quantify the contributions of these biomechanical factors; however, the high VAF values in this study nevertheless indicate that the second-order lumped element model provides a reasonable description of finger tip interactions for fast transients.

C Haptic Interface Design. For haptic interface applications, the plots showing variation of impedance parameters (Figs. 5 and 6) summarize the results. Of particular note in this context are: the near-constant value of the mass for single subjects (in the >6 N range) and small variation between subjects; the approximately linear increase in stiffness with mean force level; and the relatively large and nearly critically damped value of the damping ratio for fast transients. One important aspect of these measurements for design purposes is that they represent likely minimum values for stiffness that will be encountered in task execution. As noted above, stretch reflexes probably act to increase stiffness, as do agonist–antagonist co-contractions. Thus, at longer time scales where reflexes are significant, these measurements probably represent lower bounds to the effective stiffness.

Mechanical impedance at short time scales may be particularly important for multifinger haptic interfaces, in contrast to arm-level devices where frequencies above perhaps 2 Hz are of relatively less importance. Results presented by Howe and Kontarinis (1992) suggest that force feedback bandwidths of at least 8 Hz are helpful in teleoperated precision grasp tasks. In such high-bandwidth systems, hard surface contacts or impacts can produce rapid increases in force, where the immediate mechanical response will be described by the short time scale impedances measured here. On even shorter time scales, vibrations up to several hundred Hz in frequency form an important component of human tactile sensibility (Johansson et al., 1982). Kontarinis and Howe (1995) show that provision of high-frequency vibratory information can significantly improve performance in some telemanipulation tasks. In contrast to the findings from previous studies, these short-time scale identified parameters may facilitate the design of haptic interfaces in regimes where high frequencies are important.

The combination of both finger pad and IP joint compliances, in varying degrees for different subjects, results in nonrigid body motion of the index finger and accounts for the reduced effective mass at lower finger tip force levels. This result demonstrates that it is not sufficient for successful identification of teleoperator inertia to approximate the effective inertia of a finger by measuring its mass, because at low force levels, the effective mass loading the manipulator may indeed be less than the entire finger mass.

The results presented here identify impedance variation with a single parameter, finger tip force, and specify quantitative values for the design of haptic interfaces for teleoperation. Impedance will also vary with many other parameters, including joint angle, joint speed, co-contraction of antagonist muscles, input magnitude, and the time scale of the transient (Kearney and Hunter, 1990). For fingers in particular, the impedance can be expected to vary with the angles of other joints in the wrist or in the kinematics of the fingers themselves. In addition, a complete representation of finger impedance will require measurements of responses at longer time scales.

Acknowledgments

This paper is based on work supported by the National Science Foundation under Grant No. IRI-9357768, and the Office of Naval Research under Grant No. N00014-92-J-1887.

References

Agarwal, G. C., and Gottlieb, G. L., 1977, "Compliance of the Human Ankle Joint," ASME JOURNAL OF BIOMECHANICAL ENGINEERING, Vol. 99, pp. 166–170.

Akazawa, K., Milner, T. E., and Stein, R. B., 1983, "Modulation of Reflex EMG and Stiffness in Response to Stretch of Human Finger Muscle," *Journal of Neurophysiology*, Vol. 49, No. 1, pp. 16–27.

Amis, A. A., 1994, "The Mechanical Properties of Finger Flexor Tendons and Development of Stronger Tendon Suturing Techniques," in: *Advances in the Biomechanics of the Hand and Wrist*, F. Schuind, K. N. An, W. P. Cooney III, and M. Garcia-Elias, eds., Plenum Press, NY, pp. 41–57.

Asada, H., and Asari, Y., 1988, "The Direct Teaching of Tool Manipulation Skills via the Impedance Identification of Human Motions," *Proc. 1988 IEEE International Conference on Robotics and Automation*, Philadelphia, PA, Apr., pp. 1269–1274.

Becker, J. D., and Mote, C. D., Jr., 1990, "Identification of a Frequency Response Model of Joint Rotation," ASME JOURNAL OF BIOMECHANICAL ENGINEERING, Vol. 112, pp. 1–8.

Bennett, D. J., Hollerbach, J. M., Xu, Y., and Hunter, I. W., 1992, "Time Varying Stiffness of Human Elbow Joint During Cyclic Voluntary Movement," *Experimental Brain Research*, Vol. 88, pp. 433–442.

Cochin, I., and Plass, H. J., Jr., 1990, *Analysis and Design of Dynamic Systems*, 2nd ed., Harper Collins, New York, Chap. 2.

Colgate, J. E., and Brown, J. M., 1994, "Factors Affecting the Z-Width of a Haptic Interface," *Proc. IEEE International Conference on Robotics and Automation*, San Diego, CA, May, pp. 3205–3210.

Crowninshield, R., Pope, M. H., Johnson, R., and Miller, R., 1976, "The Impedance of the Human Knee," *Journal of Biomechanics*, Vol. 9, No. 8, pp. 529–535.

Doemges, F., and Rack, P. M. H., 1992, "Changes in the Stretch Reflex of the Human First Dorsal Interosseus Muscle During Different Tasks," *Journal of Physiology*, Vol. 447, pp. 563–573.

Dolan, J. M., Friedman, M. B., and Nagurka, M. L., 1993, "Dynamic and Loaded Impedance Components in the Maintenance of Human Arm Posture," *IEEE Transactions on Systems, Man, and Cybernetics*, Vol. 23, No. 3, pp. 698–709.

Hogan, N., 1990, "Mechanical Impedance of Single and Multi-Articulate Systems," in: *Multiple Muscle Systems: Biomechanics and Movement Organization*, J. M. Winters and S. L.-Y. Woo, eds., Springer-Verlag, New York, Chap. 9, pp. 149–164.

Howe, R. D., 1992, "A Force-Reflecting Teleoperated Hand System for the Study of Tactile Sensing in Precision Manipulation," *Proc. 1992 IEEE International Conference on Robotics and Automation*, Nice, France, May, pp. 1321–1326.

Howe, R. D., and Kontarinis, D., 1992, "Task Performance With a Dextrous Teleoperated Hand System," *Proc. SPIE*, Vol. 1833, Boston, MA, Nov., pp. 199–207.

Hunter, I. W., and Kearney, R. E., 1983, "Invariance of Ankle Dynamic Stiffness During Fatiguing Muscle Contractions," *Journal of Biomechanics*, Vol. 16, No. 10, pp. 985–991.

Johansson, R. S., Landstrom, U., and Lundstrom, R., 1982, "Responses of Mechanoreceptive Afferent Units in the Glabrous Skin of the Human Hand to Sinusoidal Skin Displacements," *Brain Research*, Vol. 244, pp. 17–25.

Jones, L. A., and Hunter, I. W., 1990a, "Dynamics of Human Elbow Joint Stiffness," CMBEC-16-CCGB, Winnipeg, pp. 175–176.

Jones, L. A., and Hunter, I. W., 1990b, "Influence of the Mechanical Properties of a Manipulandum on Human Operator Dynamics," *Biological Cybernetics*, Vol. 62, pp. 299–307.

Joyce, G. C., Rack, P. M. H., and Ross, H. F., 1974, "The Forces Generated at the Human Elbow Joint in Response to Imposed Sinusoidal Movements of the Forearm," *Journal of Physiology*, Vol. 240, pp. 351–374.

Kearney, R. E., and Hunter, I. W., 1982, "Dynamics of Human Ankle Stiffness: Variation With Displacement Amplitude," *Journal of Biomechanics*, Vol. 15, No. 10, pp. 753–756.

Kearney, R. E., and Hunter, I. W., 1990, "System Identification of Human Joint Dynamics," *Critical Reviews in Biomedical Engineering*, Vol. 18, No. 1, pp. 55–87.

Kontarinis, D. A., and Howe, R. D., 1995, "Tactile Display of Vibratory Information in Teleoperation and Virtual Environments," *Presence*, Vol. 4, pp. 387-402.

McMahon, T. A., 1984, *Muscles, Reflexes, and Locomotion*, Princeton University Press, Princeton, NJ.

Mussa-Ivaldi, F. A., Hogan, N., and Bizzi, E., 1985, "Neural, Mechanical, and Geometric Factors Subserving Arm Posture in Humans," *Journal of Neuroscience*, Vol. 5, No. 10, pp. 2732–2743.

Westling, G., and Johansson, R. S., 1987, "Responses in Glabrous Skin Mechanoreceptors During Precision Grip in Humans," *Experimental Brain Research*, Vol. 66, pp. 128–140.

Whitney, D. E., 1982, "Quasi-Static Assembly of Compliantly Supported Rigid Parts," ASME *Journal of Dynamic Systems, Measurement, and Control*, Vol. 104, pp. 65–77.